

Photomagnetothermal Effect in Semiconductors

W. W. GÄRTNER

CBS Laboratories, Stamford, Connecticut

AND

C. LOSCOE AND H. METTE

U. S. Army Signal Research and Development Laboratory, Fort Monmouth, New Jersey

(Received January 23, 1962)

The establishment of a temperature distribution in a solid by optically excited diffusing and recombining carriers has been called the photothermal (PT) effect and has previously been described by the authors for certain special cases in semiconductors. The related effect with magnetic field is called the photomagnetothermal (PMT) effect. The paper gives a formulation of the theory governing the PMT effect and the case of weak magnetic fields and small temperature elevations in an infinite slab is worked out in detail. An apparatus for measuring the effect as a function of temperature is described and experimental data are presented, giving for the first time proof of the existence of this effect in germanium. Considering the experimental difficulties the agreement between theory and measurements is quite good.

I. INTRODUCTION

THE photomagnetothermal (PMT) effect is the establishment of a temperature distribution in a solid by optically excited diffusing and recombining carriers in the presence of a magnetic field. In the simplest case, depicted in Fig. 1, the directions of light incidence, magnetic field, and measured PMT temperature gradient are mutually perpendicular. The PMT effect may be regarded as a modification—caused by the influence of the magnetic field on the carrier diffusion—of the photothermal (PT) effect which has previously been described by the authors.^{1,2} While recombination-heat effects under the influence of a magnetic field due to thermally generated carriers have been previously investigated,³⁻⁵ no recombination-heat effect involving optically generated carriers has to our knowledge been reported. The present experimental investigation of the

photomagnetothermal effect in germanium, therefore, constitutes for the first time proof of the existence of such an optical recombination-heat effect.

II. THEORY

The general theory of the PMT effect is quite complicated and a basic formulation has been given.² We shall restrict ourselves here to the discussion of a simple case which, however, illustrates the salient features of the effect and is also amenable to experimental verification.

PMT Effect in the Infinite Slab (Fig. 2)

According to Eq. (II.5) of reference 2, the energy flux \mathbf{f}_P associated with a density of excess carriers is given by

$$\mathbf{f}_P = E_G(\mu_n n_0 \mathbf{j}_p - \mu_p p_0 \mathbf{j}_n) / \sigma_0, \quad (1)$$

where $\sigma_0 = q\mu_n n_0 + q\mu_p p_0$ is the equilibrium conductivity of the sample. With the magnetic field in the z direction (Fig. 1) this energy flux in general has an x and a y component. The temperature distribution in the sample then depends on the boundary conditions for the total heat flux and for the temperature. As a simple case, we may assume that no energy flows through the sample in the x and z directions, i.e., in particular,

$$\int_0^w f_{ix} dy = 0, \quad (2)$$

where f_{ix} is the x component of the total internal heat flux. We assume that in the simplest case it consists only of f_{Px} and the lattice thermal conductivity:

$$f_{ix} = f_{Px} - \kappa(\partial T / \partial x), \quad (3)$$

where T is the temperature and κ is the customary thermal conductivity of the lattice and the equilibrium carriers. Substituting (3) into (2), one obtains

$$\int_0^w f_{Px} dy = \kappa \int_0^w (\partial T / \partial x) dy. \quad (4)$$

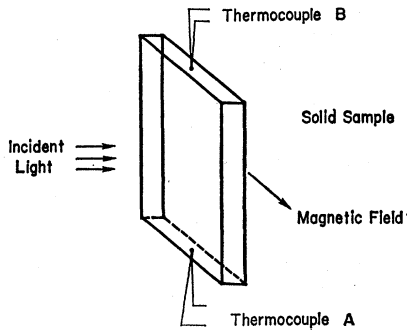


FIG. 1. Typical experimental arrangement for the investigation of the PMT effect. The PMT temperature difference is measured between thermocouples A and B.

¹ W. W. Gärtner, H. Mette, and C. Loscoe, *Bull. Am. Phys. Soc.* **6**, 28 (1961).

² W. W. Gärtner, *Phys. Rev.* **122**, 419 (1961).

³ H. Mette, W. W. Gärtner, and C. Loscoe, *Phys. Rev.* **115**, 537 (1959).

⁴ H. Mette, W. W. Gärtner, and C. Loscoe, *Phys. Rev.* **117**, 1491 (1960).

⁵ B. V. Paranjape and J. S. Levinger, *Phys. Rev.* **120**, 437 (1960).

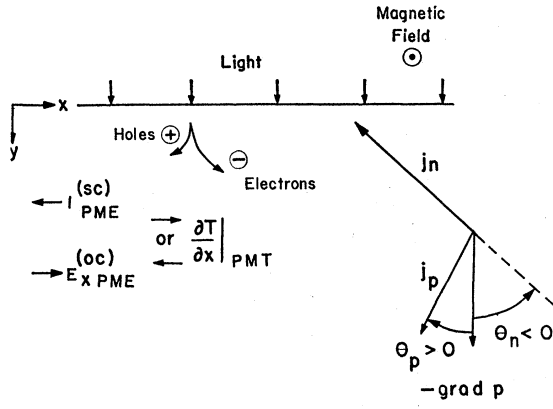


FIG. 2. The photomagnetothermal effect in an infinite semiconductor slab.

If one assumes that the PT temperature gradient $(\partial T/\partial y)$ is independent of x and z , i.e.,

$$\frac{\partial}{\partial x} \left(\frac{\partial T}{\partial y} \right) = \frac{\partial}{\partial z} \left(\frac{\partial T}{\partial y} \right) = 0, \quad (5)$$

it follows from $\text{curl grad } T = 0$ that

$$\frac{\partial}{\partial y} \left(\frac{\partial T}{\partial x} \right) = 0, \quad (6)$$

and one finds with Eq. (4) that

$$\frac{\partial T}{\partial x} = \frac{1}{\kappa w} \int_0^w f_{Px} dy, \quad (7)$$

and with (1) that

$$\frac{\partial T}{\partial x} = \frac{E_G}{\kappa w \sigma_0} \int_0^w (\mu_n n_0 j_{Px} - \mu_p p_0 j_{Nx}) dy. \quad (8)$$

To calculate the PMT temperature gradient it is thus necessary to find expressions for j_{Px} and j_{Nx} under the prevailing conditions.

For small Hall angles, one finds according to van Roosbroeck⁶

$$j_{Px} = j_{Px}^* + \theta_p (\mathbf{j}_p^* \times \mathbf{k})_x = j_{Px}^* + \theta_p j_{Py}^* \quad (9)$$

and

$$j_{Nx} = j_{Nx}^* + \theta_n (\mathbf{j}_n^* \times \mathbf{k})_x = j_{Nx}^* + \theta_n j_{Ny}^*, \quad (10)$$

where θ_p and θ_n are the Hall angles for holes and electrons, respectively, and

$$\mathbf{j}_p^* = \sigma_p \mathbf{E} - q D_p \text{grad } p, \quad (11)$$

$$\mathbf{j}_n^* = \sigma_n \mathbf{E} + q D_n \text{grad } n, \quad (12)$$

where $\sigma_p = q \mu_p p$, $\sigma_n = q \mu_n n$, and \mathbf{E} is the electric field. Considering that under the assumption of local charge

neutrality $\text{grad } p = \text{grad } n$, and that the Demer voltage E_y is given by⁷

$$E_y = -q \frac{D_n - D_p}{\sigma} \frac{\partial p}{\partial y} \quad (13)$$

(with $\sigma = \sigma_n + \sigma_p$), one finds

$$j_{Py}^* = -j_{Ny}^* = -(q/\sigma) (\sigma_p D_n + \sigma_n D_p) (\partial p / \partial y). \quad (14)$$

Since in the infinite slab with small temperature differences $(\partial p / \partial x) = (\partial n / \partial x) = 0$, one obtains

$$j_{Px} = \sigma_p E_x - \theta_p (q/\sigma) (\sigma_p D_n + \sigma_n D_p) (\partial p / \partial y), \quad (15)$$

$$j_{Nx} = \sigma_n E_x + \theta_n (q/\sigma) (\sigma_p D_n + \sigma_n D_p) (\partial p / \partial y). \quad (16)$$

Substituting Eqs. (15) and (16) into integral (8) yields

$$\begin{aligned} \frac{\partial T}{\partial x} &= \frac{E_G}{\kappa w \sigma_0} (\sigma_n \mu_p - \sigma_p \mu_n) E_x \int_0^w \Delta p dy \\ &\quad - \frac{E_G}{\kappa w \sigma_0} (\sigma_n \theta_p + \sigma_p \theta_n) \int_0^w \frac{\sigma_p D_n + \sigma_n D_p}{\sigma} \frac{\partial p}{\partial y} dy. \end{aligned} \quad (17)$$

Since the photoconductance ΔG of the illuminated slab per unit width along the magnetic field and unit length in the x direction is given by

$$\Delta G = q (\mu_p + \mu_n) \int_0^w \Delta p dy, \quad (18)$$

and the photomagnetoelectric (PME) short-circuit current $I_{\text{PME}}^{(\text{sc})}$ per unit width along the magnetic field is equal to [see reference 6, Eq. (37)]

$$I_{\text{PME}}^{(\text{sc})} = -(\theta_p - \theta_n) q \int_0^w \frac{\sigma_n D_p + \sigma_p D_n}{\sigma} \frac{\partial p}{\partial y} dy, \quad (19)$$

one may rewrite Eq. (17) as

$$\begin{aligned} \frac{\partial T}{\partial x} &= \frac{E_G}{\kappa w \sigma_0 q} \frac{\sigma_n \mu_p - \sigma_p \mu_n}{\mu_p + \mu_n} E_x \Delta G \\ &\quad + \frac{E_G}{\kappa w \sigma_0 q} \frac{\sigma_n \theta_p + \sigma_p \theta_n}{\theta_p - \theta_n} I_{\text{PME}}^{(\text{sc})}. \end{aligned} \quad (20)$$

We may now distinguish the two cases of electrical short and open circuit. In the first case where

$$E_x = 0 \quad (21)$$

one obtains

$$\left. \frac{\partial T}{\partial x} \right|_{\text{sc}} = \frac{E_G}{\kappa w \sigma_0 q} \frac{\sigma_n \theta_p + \sigma_p \theta_n}{\theta_p - \theta_n} I_{\text{PME}}^{(\text{sc})}. \quad (22)$$

Considering that for weak magnetic fields the Hall angles are proportional to the magnetic field one ob-

⁶ W. van Roosbroeck, Phys. Rev. **101**, 1713 (1956), Eq. (13).

⁷ W. W. Gärtner, Phys. Rev. **105**, 823 (1957), Eq. (18).

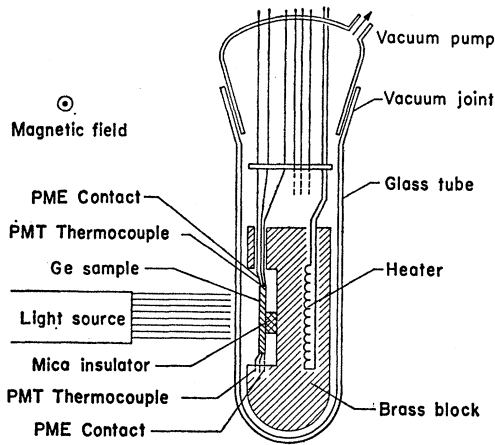


Fig. 3. Apparatus for measuring PME and PMT effects.

serves that the ratio of the PMT temperature gradient over the PME short-circuit current is independent of light intensity, magnetic field, lifetime, and surface recombination velocities.

In the open-circuit case, one finds

$$\left. \frac{\partial T}{\partial x} \right|_{oc} = \frac{E_G}{\kappa w \sigma_0 q} \left[\frac{\sigma_{n0} \mu_p - \sigma_{p0} \mu_n}{\mu_p + \mu_n} \Delta G - \frac{\sigma_{n0} \theta_p + \sigma_{p0} \theta_n}{\theta_p - \theta_n} G \right] E_{x \text{ PME}^{(oc)}}, \quad (23)$$

since the open circuit PME field $E_{x \text{ PME}^{(oc)}}$ and the short-circuit PME current $I_{\text{PME}^{(sc)}}$ are related by the equation

$$I_{\text{PME}^{(sc)}} = -G E_{x \text{ PME}^{(oc)}} \quad (24)$$

[see reference 6, Eq. (39)], where G is the conductance of the illuminated slab per unit width along the magnetic field and unit length in the x direction.

In the small-signal case where the photoconductivity is everywhere small compared with the equilibrium conductivity, the influence of the photoconductance in Eq. (23) is small and the ratio of PMT temperature gradient over PME open-circuit voltage is again independent of light intensity, magnetic field, lifetime, and surface recombination velocity. It is therefore relatively easy to compare measured values of these ratios with theoretical predictions.

From Eqs. (22) and (23) which hold for surface and for bulk generation of carriers one observes the general characteristics of the PMT effect:

The temperature gradient has different signs for p - and n -type materials of the same lifetime, surface recombination velocities, and illumination conditions. Its dependence on the wavelength of the incident light follows the spectral distribution of the PME effect as derived in reference 7. The ratio of PMT temperature gradient over PME open-circuit voltage or short-circuit current is largest in low-resistivity samples. Upon ap-

proach to intrinsic conditions, n - or p -type samples undergo a sign change depending on the relative magnitude of drift and Hall mobilities for electrons and holes.

Figure 4(a) shows the theoretical ratio of PMT temperature difference over PME voltage as a function of temperature for the small-signal case as given by Eq. (23). The numerical values of the various parameters are the same as those used in reference 3.

III. EXPERIMENT

From the above considerations it follows that the PMT effect is largest in materials capable of producing a high PME current. Since the highest PME effect so far has been measured in germanium,⁸ only this material was used for the present investigation. The experimental apparatus is shown in Fig. 3.

The samples were slabs, 2 cm long, 0.7 cm wide, and about 0.5 mm thick of single-crystal germanium. Before being mounted, each sample was washed in alcohol and then in distilled water, etched in a mixture of half nitric and half hydrofluoric acids until shiny, and then rinsed thoroughly in distilled water. The surface selected to be the back surface was rubbed with fine sandpaper. This insures low recombination at the front surface and high recombination at the back.

With the etched (shiny) side up, the sample was fastened with a drop of sauerisen cement to a thin sheet of mica which in turn was cemented to a brass block. The brass block was provided with heating coils so that the sample temperature could be raised. Tiny (0.002-in. diameter) copper-Constantan thermocouples were used in order to minimize as much as possible errors in thermocouple readings due to the magnetic field.⁹ The thermocouples allowed the measurement of both the PMT temperature difference and the absolute temperature of the sample. The PME voltage was measured with copper leads (0.010-in. diameter), that were attached to the ends of the sample by a small dab of silver paint and checked for ohmic contacts.

Oxidation of the etched sample surface, even at room temperature, changes considerably the recombination rate of the etched surface and, therefore, the PMT and PME effects. To minimize such changes during the temperature runs, the mounted sample was put into a glass tube which was evacuated throughout the experiment. The tube was fitted at its top with a ground joint so that it could be easily opened to exchange samples. All thermocouple and lead wires left the tube through the top, the openings made airtight by melting sealing wax into them. A radiation shield made of aluminum foil enclosed the tube except for a hole, the size of the sample, through which the light from a microscope lamp

⁸ A. Boatright, H. Mette, and E. Ahlstrom, "1961 Electron Devices Meeting, IRE, PGED," Washington, D. C., October 26-28, 1961 (unpublished).

⁹ C. Loscoe and H. Mette, *Temperature, Its Measurement and Control in Science and Industry* (Reinhold Publishing Corporation, New York, 1962), Vol. 3, Chap. 23.

TABLE I. Measured values of PMT temperature difference (for opposite directions of magnetic field) at 12 400 gauss and 45°C ambient temperature for six different samples, all 2 cm long.

Resistivity (at room temperature) (ohm cm)	Type	PMT temperature difference (degrees)
1.0	<i>p</i>	+0.075
5.2	<i>p</i>	+0.045
50	<i>p</i>	-0.006
5.6	<i>n</i>	-0.024
2.6	<i>n</i>	-0.022
0.87	<i>n</i>	-0.051

was focused on the sample. The shield also masked the thermocouple and the PME leads from the light. The tube was then placed between the poles of an electromagnet. The direction of the magnetic field was perpendicular to the plane of the diagram in Fig. 3.

Measurements of the PMT temperature difference and the PME voltage were made on both *p*- and *n*-type samples of various resistivities from room temperature to 150°C at a magnetic field strength of 12 400 gauss. This high field strength was necessary to bring the PMT effect into an experimentally accessible range. Although the PMT effect at these field strengths is no longer expected to be linear with the magnetic field, its deviation from linearity is not expected to be larger than the 20 to 30% that were previously measured for the Nernst³ and PME⁸ effects in germanium. The PMT temperature difference was measured by a Keithley Instruments model 149 millimicrovoltmeter connected between the two thermocouples. At each temperature the direction of the magnetic field was reversed every 30 sec and the meter readings recorded for a period of 10 min. These readings were plotted and averaged graphically. In this way any error arising from the drifting of the ambient temperature was eliminated. Thirty seconds between reversals of the field were found to be sufficient time for the sample to reach thermal equilibrium.

A direct comparison among the measured values of the PMT temperature difference for the same sample at various temperatures and for samples of different resistivities is difficult because surface conditions, and therefore recombination velocities, are not reproducible experimentally. However, an indication of the size of the PMT temperature difference can be obtained from the chart in Table I. It shows measured values (for opposite directions of the magnetic field and, therefore, double the effect) at 12 400 gauss, 45°C ambient temperature, and high light intensities for six samples with different resistivities, all 2 cm long.

The PME open-circuit voltage was measured at the same temperature as the PMT effect by means of a Hewlett-Packard millivoltmeter. Figure 4 shows measured values of the ratio of PMT temperature difference over PME open-circuit voltage—which is independent of light intensity and surface recombination velocities, and therefore easier to measure—as a function of tem-

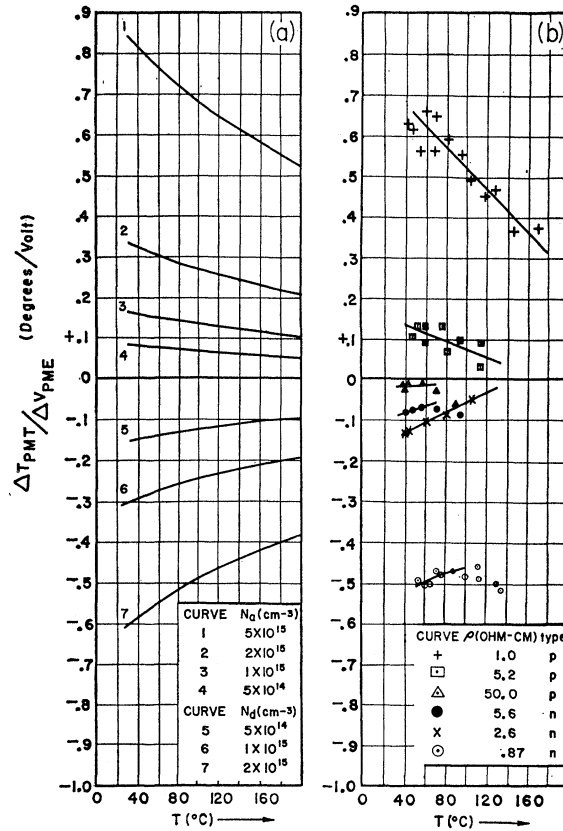


FIG. 4. Ratio of PMT temperature gradient over PME open-circuit field for *p*- and *n*-type germanium with various impurity concentrations as a function of temperature: (a) theoretical; (b) experimental at 12 400 gauss.

perature from room temperature to 150°C for several *p*- and *n*-type germanium samples of different resistivities.

IV. COMPARISON BETWEEN THEORY AND EXPERIMENT

Figure 4 compares the theory of the PMT effect with the measured values. In view of the limited accuracy of the measurements due to the very small size of the PMT effect, the agreement between theory and experiment is quite satisfactory. It is seen that as predicted from Eq. (23) the PMT/PME ratio is large for low-resistivity samples and small for high-resistivity samples. It is also clear that the sign of the ratio (as usually determined by the sign of the PMT effect) is positive for extrinsic *p*-type material and negative for extrinsic *n*-type material. In intrinsic germanium samples the sign is negative due to the fact that the ratio of electron over hole drift mobility is higher than the ratio of electron over hole Hall mobility.

The following small discrepancies between theory and experiment are noticed:

In the 50-ohm-cm *p*-type sample the sign of the PMT effect is already negative although theoretically the sign

change would be expected at somewhat lower carrier densities.

The experimental curves are found to decrease more rapidly with increasing temperature than the theoretical ones.

In some samples the experimental values begin to increase again at higher temperatures.

Whether these deviations have real significance or are the result of systematic errors cannot be determined

from the present experiments, especially since the PME effect decreases rapidly with increasing temperature.¹⁰

ACKNOWLEDGMENT

It is a pleasure to acknowledge an informative discussion with W. van Roosbroeck of Bell Telephone Laboratories.

¹⁰ S. Goldstein, H. Mette, and W. W. Gärtner, *J. Phys. Chem. Solids* **8**, 78 (1959).

PHYSICAL REVIEW

VOLUME 126, NUMBER 5

JUNE 1, 1962

Sharp-Line Fluorescence, Electron Paramagnetic Resonance, and Thermoluminescence of Mn^{4+} in $\alpha\text{-Al}_2\text{O}_3$

S. GESCHWIND, P. KISLIUK, M. P. KLEIN,* J. P. REMEIK, AND D. L. WOOD
Bell Telephone Laboratories, Inc., Murray Hill, New Jersey

(Received January 15, 1962)

Sharp-line fluorescence, paramagnetic resonance in the ground state, and optical absorption due to Mn^{4+} in $\alpha\text{-Al}_2\text{O}_3$ have been observed (analog of Cr^{3+}). The Mn^{4+} valence state is obtained by charge compensation with Mg^{2+} . The increased charge of Mn^{4+} compared to Cr^{3+} results in a stronger crystal field and greater covalency whose effects are clearly seen in both the optical and paramagnetic resonance results. The ground state splitting is 0.39 cm^{-1} , almost the same as in ruby, while the metastable 2E state splitting is 80 cm^{-1} . When the crystals are irradiated with ultraviolet ($<3000\text{ Å}$), more than 50% of the ground state of Mn^{4+} is depopulated, as long-lived traps are filled which decay via the 2E states through sharp-line thermoluminescence. The possible application to light masers is briefly discussed.

WE have observed sharp-line fluorescence, paramagnetic resonance in the ground state, and optical absorption due to Mn^{4+} in $\alpha\text{-Al}_2\text{O}_3$ (analog of Cr^{3+}). Also, in initial experiments more than 50% of the Mn^{4+} ground state has been depopulated by ultraviolet irradiation, filling long-lived traps which decay via the 2E states through sharp-line thermoluminescence. This paper is a preliminary report of our findings whose intent is to draw attention only to the main properties of the system. A more detailed presentation will appear in a subsequent publication.

Single crystals of $\alpha\text{-Al}_2\text{O}_3\text{-Mn}^{4+}$ were grown from oxide fluxes to which it was found necessary to add MgO powder to provide Mg^{2+} to charge compensate the Mn^{4+} which enters substitutionally into the octahedral Al^{3+} site. Similar results were obtained with Mg^{2+} compensated crystals grown by the Linde Company by the flame fusion process. The concentration of Mn^{4+} in our experiments varied from about 0.1% to 0.001%. While reference may be found in the phosphor literature^{1,2} to Mn^{4+} in Al_2O_3 , the description of the optical and mag-

netic properties has been greatly extended and clarified in this work.

The Mn^{4+} ion is isoelectronic with Cr^{3+} ($3d^3$ configuration) and the electronic states of the latter ion

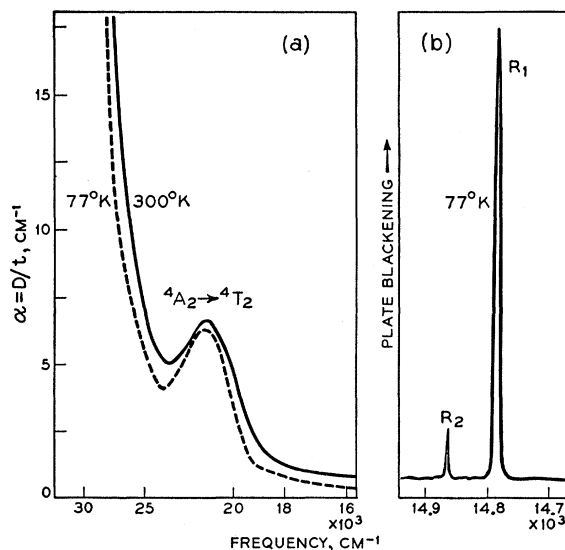


FIG. 1. Absorption (a) and fluorescence (b) spectra of $\text{Al}_2\text{O}_3\text{-Mn}^{4+}$ grown from flux. Concentration: less than 0.08% Mn^{4+} by weight. The curve in (b) is a microphotometer trace giving a nonlinear ordinate.

* Now at the University of California, Lawrence Radiation Laboratory, P. O. Box 808, Livermore, California.

¹ P. Pringsheim, *Fluorescence and Phosphorescence* (Interscience Publishers, Inc., New York, 1949) who quotes E. Tiede and R. Piwonka, *Chem. Ber.* **64**, 2252 (1931).

² F. A. Kröger, *Some Aspects of the Luminescence of Solids* (Elsevier Publishing Company, Inc., Amsterdam, Netherlands, 1948).